

Uniform trace formulae for $SU(2)$ and $SO(3)$ symmetry breaking

M. Brack, P. Meier and K. Tanaka^{*)}

Institut für Theoretische Physik, Universität Regensburg, D-93040 Regensburg, Germany

Abstract

We develop uniform approximations for the trace formula for non-integrable systems in which $SU(2)$ symmetry is broken by a non-linear term of the Hamiltonian. As specific examples, we investigate Hénon-Heiles type potentials. Our formalism can also be applied to the breaking of $SO(3)$ symmetry in a three-dimensional cavity with axially-symmetric quadrupole deformation.

PACS number: 03.65.Sq

November 5, 1998

J. Phys. **A**, in print

^{*)} *Present address:* Department of Physics, University of Alberta, Edmonton, Alberta, Canada T6G 2J1.

1 Introduction

Systems with mixed classical dynamics have so far offered the most difficult problems in the attempts of a semiclassical quantization in terms of periodic orbits [1, 2, 3, 4]. These problems have mainly three origins: 1) the existence of continuous symmetries that make (some of) the periodic orbits non-isolated, 2) bifurcations of stable orbits, and 3) the proximity of a higher symmetry that is reached by letting a continuous parameter go to zero. In all three cases, the original trace formula of Gutzwiller [1] cannot be used because the stationary-phase integration transverse to the periodic orbits, that is used in its derivation, is not justified and leads to divergences. By now, the problems connected to 1) and 2) are essentially solved. Besides fully integrable systems [2, 3], non-integrable systems with various kinds of continuous symmetries can also be treated by properly extended versions of the Gutzwiller theory [5, 6]. Considerable progress has also been made recently in the treatment of bifurcations, after earlier indications how to go beyond the simplest saddle-point integration [2, 3, 7]. Sieber and Schomerus [8, 9] have systematically developed uniform approximations to the most common types of bifurcations, expanding the action integrals in the neighborhood of a bifurcation point into normal forms in phase space [10]. The resulting trace formulae interpolate continuously between the appropriate Gutzwiller limits that are sufficiently far away from the bifurcation points, where the stationary-phase integration can be applied.

In the present paper, we shall be concerned with the third type of problems which arise from the breaking of a given symmetry through a continuous parameter in the Hamiltonian. Let us start from an integrable system described by a Hamiltonian H_0 which possesses a certain continuous symmetry. As a consequence of this symmetry, the periodic orbits in the classical system occur in degenerate families living on N -tori in phase space, where N is the number of degrees of freedom of the integrable system. We now perturb the system by adding to it a term that breaks the symmetry:

$$H = H_0 + \epsilon H_1. \quad (1)$$

Here ϵ is a continuous dimensionless parameter which in the following we may also call a “deformation”. Due to the symmetry breaking, some (or all) of the rational tori containing the periodic orbit families are broken up into orbits that have a lesser degree of degeneracy than those of H_0 , or are completely isolated. The system (1) will in general exhibit mixed classical dynamics, and if H_1 breaks all continuous symmetries of H_0 , it will become chaotic for large values of ϵ and for large energies, where the standard Gutzwiller trace formula can be applied. However, for small ϵ the amplitudes in this formula become very large; they actually diverge for $\epsilon \rightarrow 0$. This is due to the fact that although the rational tori are broken up for $\epsilon > 0$, the periodic orbits are still not sufficiently isolated as long as their perturbed actions differ by less than \hbar , and consequently the stationary-phase integration transverse to the orbits fails as mentioned above. One then has to find more accurate ways of performing the trace integration over the semiclassical Green’s function; in principle, closed non-periodic orbits will thereby also contribute significantly to the result [11].

In the limit of small perturbations, $\epsilon \ll 1$, classical perturbation theory may be used to derive trace formulae with finite amplitudes that yield the correct limit for $\epsilon \rightarrow 0$. Generalizing earlier attempts [12, 13], Creagh [14] has recently developed a scheme to derive perturbative trace formulae for the breaking of arbitrary continuous symmetries, including e.g. $SO(3)$ (spherically symmetric potentials) or $SU(N)$ (harmonic oscillators in N dimensions). Applications of

this approach have been presented in Refs. [15, 16, 17, 18]. The results successfully describe the transitions from higher to lower (or no) symmetry for small or moderate deformations ϵ , but they eventually fail when the perturbative regime is exceeded. In the limit of large perturbation, $\epsilon \gg 1$, one would like to recover the Gutzwiller trace formula [1] for isolated orbits, or its corresponding extension [5, 6] if some continuous symmetries are left. A closed form of an approximation that yields this limit as well as the correct trace formula of the integrable system H_0 for $\epsilon \rightarrow 0$ is called a uniform approximation, in analogy to the uniform approximations that interpolate continuously across bifurcations.

Tomsovic, Grinberg, and Ullmo [19] have recently derived a uniform approximation for the breaking of U(1) symmetry in a two-dimensional system. Their result is quite general and applies to all systems where the rational tori are broken into pairs of stable and unstable isolated orbits. No analogous result is known to us for the breaking of a higher symmetry in any dimension. We will discuss the approach of Ref. [19] briefly in Sect. II and rederive it from the perturbative limit in a heuristic way that is suitable for an extension to higher symmetries of H_0 .

In this paper, we derive uniform approximations to perturbed harmonic oscillators in two dimensions, where H_0 has SU(2) symmetry (Sect. III). We furthermore apply one of the results to a three-dimensional cavity with small axially-symmetric quadrupole deformations, where one starts from SO(3) symmetry (Sect. IV).

Our aim is not the full quantization of these systems, but the description of their gross-shell properties which are determined by the shortest orbits [4, 5]. The use of the periodic orbit theory to describe shell effects in many-fermion systems in terms of a few short orbits has found nice applications, e.g., in nuclei, for ground-state deformations [20] and the mass asymmetry of fission [21]; in metal clusters, for supershells [22] and (using the perturbative approach [14]) their modifications due to deformations [15, 16] and magnetic fields [17]; and in semiconductor quantum dots, for magnetization [13, 23] and conductance fluctuations [16, 24].

2 Recapitulation of U(1) breaking

We start by recapitulating the work of Tomsovic *et al.* [19] for the breaking of U(1) symmetry in a two-dimensional system. We shall re-derive here their result in the simplified version given by Sieber [9], using a heuristic way which will be generalized in the later sections to systems with higher symmetries.

We restrict ourselves to the most frequently occurring case that a periodic orbit family on a 2-torus is broken into a non-degenerate pair of stable and unstable isolated orbits. In the two-dimensional trace integral, one integration is performed exactly along the orbits as usual. The space variable q transverse to the orbit can always be mapped onto a variable ϕ which is cyclic in $[0, 2\pi)$ and as a function of which the action shift is proportional to $\cos(\phi)$ (“pendulum mapping” in [19]). Hence the contribution of an orbit family to the trace formula is

$$\delta g = \Re e \left\{ e^{i\Phi_0} \frac{1}{2\pi} \int_0^{2\pi} A(\phi) \mathcal{J}(\phi) e^{\frac{i}{\hbar} \delta S \cos(\phi)} d\phi \right\}. \quad (2)$$

Here $A(\phi)$ is the Gutzwiller amplitude function in the trace formula for the perturbed system, $\mathcal{J}(\phi) = \partial q / \partial \phi$ is the Jacobian due to the variable mapping, and $\Phi_0 = S_0 / \hbar - \sigma_0 \pi / 2$ is the overall phase (including the action S_0 and the Maslov index σ_0) of the level density in the unperturbed

system with $U(1)$ symmetry. The quantity $\delta S \cos(\phi)$ in the exponent is the action shift caused by the symmetry breaking term in the Hamiltonian. For a first inspection, perturbation theory might give a hint to the value of the constant δS (which depends on the energy and on the parameters in the symmetry breaking term, such as deformation, nonlinearity, etc.). Hereby one may have to go beyond the first order of the perturbation expansion. Recent work on Hénon-Heiles systems [18] gives us a hint that going to the lowest order at which δS becomes nonzero – however high it may be – can be combined with keeping the unperturbed amplitude A_0 . Putting $A(\phi)\mathcal{J}(\phi) = A_0$, which one may do in the small-perturbation limit, the ϕ integral in (2) can be done analytically, and one obtains

$$\delta g = A_0 J_0(\delta S/\hbar) \cos(\Phi_0), \quad (3)$$

where $J_0(x)$ is a standard cylindrical Bessel function. When δS is zero, we have the trace formula in the symmetric limit (for one orbit family)

$$\delta g_0 = A_0 \cos(\Phi_0) = A_0 \cos(S_0/\hbar - \sigma_0 \pi/2). \quad (4)$$

For large deviations from the $U(1)$ symmetry, i.e., for $\delta S \gg \hbar$, we can use the asymptotic expansion of $J_0(x) \sim \sqrt{(2/\pi|x|)} \cos(x - \pi/4)$ to find

$$\delta g \sim A_0 \sqrt{\hbar/2\pi|\delta S|} [\cos(\Phi_0 + \delta S/\hbar - \pi/4) + \cos(\Phi_0 - \delta S/\hbar + \pi/4)]. \quad (5)$$

This corresponds to the two isolated orbits with the action shifts $\pm \delta S$ and the corresponding corrections to the Maslov indices. Note that the two terms above arise from a saddle-point approximation to the integral in (2) at the stationary points $\phi_0 = 0$ and $\phi_0 = \pi$, respectively. The action shifts and amplitudes in (5) will in general be correct only in the small-perturbation limit.

We want to find a uniform approximation that for $\delta S \gg \hbar$ reaches the correct Gutzwiller trace formula for the pair of isolated orbits

$$\delta g_G = A_u \cos(S_u/\hbar - \sigma_u \pi/2) + A_s \cos(S_s/\hbar - \sigma_s \pi/2), \quad (6)$$

where the indices s and u refer to the stable and unstable orbits, respectively. We first define the following quantities:

$$\bar{A} = \frac{1}{2}(A_u + A_s), \quad \Delta A = \frac{1}{2}(A_u - A_s), \quad \bar{S} = \frac{1}{2}(S_u + S_s), \quad \Delta S = \frac{1}{2}(S_u - S_s), \quad (7)$$

$$\bar{\Phi} = \bar{S}/\hbar - \bar{\sigma}, \quad \bar{\sigma} = \frac{1}{2}(\sigma_u + \sigma_s) = \sigma_0. \quad (8)$$

We now make the following ansatz for the uniform approximation, which consists of expanding the product $A(\phi)\mathcal{J}(\phi)$ up to two terms with suitably chosen coefficients:

$$\delta g_u = \sqrt{2\pi|\Delta S|/\hbar} \Re \left\{ e^{i\bar{\Phi}} \frac{1}{2\pi} \int_0^{2\pi} (\bar{A} + \Delta A \cos \phi) e^{\frac{i}{\hbar} \Delta S \cos(\phi)} d\phi \right\}. \quad (9)$$

For small perturbations, $\Delta S \sim \delta S$, and therefore (9) will by construction lead to the correct symmetric limit (4), since the divergence of the Gutzwiller amplitudes in this limit is given by

the first factor in Eq. (5). On the other hand, the coefficients in parentheses under the integral in (9) have been chosen such that in the asymptotic limit $|\Delta S| \gg \hbar$, the stationary-phase evaluation will lead to the amplitudes $\bar{A} \pm \Delta A$ which are precisely the Gutzwiller amplitudes A_u and A_s , respectively, and thus give the form (6).

The integration in (9) can be done analytically, using

$$\frac{1}{2\pi} \int_0^{2\pi} d\phi \cos \phi e^{ix \cos \phi} = iJ_1(x), \quad (10)$$

and leads to the Tomsovic-Grinberg-Ullmo (TGU) uniform approximation [19], in the compact form given by Sieber [9], for the contribution of a pair of symmetry-broken isolated orbits to the trace formula:

$$\delta g_u = \sqrt{2\pi|\Delta S|/\hbar} \left\{ \bar{A} J_0(\Delta S/\hbar) \cos(\bar{\Phi}) - \Delta A J_1(\Delta S/\hbar) \sin(\bar{\Phi}) \right\}. \quad (11)$$

Note that this formula holds for all generic non-integrable systems in two dimensions that arise from an integrable system with U(1) symmetry through a symmetry-breaking term in the Hamiltonian that is governed by a continuous parameter. Particular examples are two-dimensional billiards obtained by deforming the circular billiard. The nature of the deformation parameter generally plays no role. The only assumption made is that the original orbit families (i.e., polygons in the case of the circular billiard) are broken into pairs of stable and unstable isolated orbits. The modification that becomes necessary when extra degeneracies due to discrete symmetries are present is trivial and will be dealt with explicitly in the examples discussed below. The breaking into orbit pairs is the most frequent situation. Exceptions occur, e.g., in billiards with octupole or hexadecapole deformations, where the boundary in polar coordinates is given by $r(\theta) = R[1 + \epsilon_\ell P_\ell(\cos \theta)]$ with $\ell = 3$ or 4. There the diameter orbit family breaks up into more than two isolated librating orbits (not counting discrete degeneracies) [25]. These have to be treated with different (and more complicated) uniform approximations.

We also note that the deformation away from the integrable case should be small enough that no bifurcation of the stable isolated orbits has taken place or is about to arise. Near the bifurcation points, the known uniform approximations apply [7, 8, 9] which we shall not discuss here.

3 Uniform approximations for SU(2) breaking

No uniform approximation has, to our knowledge, been derived so far for systems with higher than U(1) symmetry. In the following, we shall do so for two systems obtained by breaking the SU(2) symmetry of the two-dimensional harmonic oscillator. We shall follow the heuristic way of deriving the uniform approximation described in the previous section, starting from the perturbative limit which here is treated using the approach of Creagh [14].

For isotropic and anisotropic harmonic oscillators in any dimension, analytical trace formulae are known which converge to the exact quantum-mechanical sum of delta functions [4, 26]. For the two-dimensional isotropic case, the oscillating part of the level density is

$$\delta g_0 = A_0 \sum_{r=1}^{\infty} \cos\left(\frac{rS_0}{\hbar}\right), \quad A_0 = \frac{2E}{(\hbar\omega)^2}, \quad S_0 = \frac{2\pi E}{\omega}. \quad (12)$$

(Note that the smooth Thomas-Fermi part is given by $A_0/2$.) As pointed out in [14], the continuous degeneracy of the classical periodic orbits in this system can be described by integration of the surface element $d\Omega = \sin \beta d\beta d\gamma$ of a unit sphere:

$$\frac{1}{4\pi} \int_0^{2\pi} d\gamma \int_0^\pi \sin \beta d\beta = 1. \quad (13)$$

As a result of the $SU(2)$ symmetry, the action S_0 is independent of the angles β and γ . In the presence of a small perturbation, the periodic orbits will be distorted, resulting in an action shift δS that in general will depend on β and γ . Explicit ways of calculating $\delta S(\beta, \gamma)$ starting from a Hamiltonian of the form (1) are given in [14]. For small values of the perturbation parameter ϵ , the main effects governing the level density will come from the action shift in the phase of the trace formula, whereas the unperturbed amplitude A_0 can be retained. The perturbative trace formula for symmetry breaking then reads as

$$\delta g_{pert} = A_0 \Re \left\{ \sum_{r=1}^{r_m} \mathcal{M}(rx) e^{irS_0/\hbar} \right\}. \quad (14)$$

Here the modulation factor $\mathcal{M}(x)$ (which in general is complex) is given by the average of the phase shift, taken over the originally degenerate periodic orbit family,

$$\mathcal{M}(x) = \frac{1}{4\pi} \int_0^{2\pi} d\gamma \int_0^\pi \sin \beta d\beta e^{i\delta S(\beta, \gamma)/\hbar}, \quad (15)$$

and r is the repetition number. The dimensionless quantity x is proportional to ϵ and inversely proportional to \hbar , and depends on some power of the energy E . For $\epsilon \rightarrow 0$ and hence $x \rightarrow 0$, we have $\delta S \rightarrow 0$ so that $\mathcal{M} \rightarrow 1$, and the unperturbed trace formula (12) is recovered. The repetition number r in (14) cannot be summed up to arbitrarily high values, since the argument rx must remain of order unity or smaller for the perturbation approach to be valid. Hence, the maximum value r_m must be chosen such that $r_m x \lesssim 1$ for given values of ϵ and E . This excludes in general the possibility of quantizing the system through the trace formula in this approach. However, we shall be interested only in the low-frequency components of the oscillating level density, i.e., in its gross-shell structure that is governed by the shortest periodic orbits and their first few repetitions [4, 5].

Our main task now is to generalize the modulation factor (15) in such a way that the trace formula (14) goes over to the Gutzwiller formula [1] for isolated orbits in the limit of large perturbations ϵ that fully break the symmetry, whereas the limit $\mathcal{M}(0) = 1$ is preserved. If we succeed in finding such a generalization, it will smoothly interpolate between the exact trace formula (12) for the harmonic oscillator and the Gutzwiller formula for the symmetry-broken limit, and hence be a suitable uniform approximation. Note that Eq. (14) with (15) is exactly of the same form as Eq. (2) for the $U(1)$ case, except that we now have a two-fold integral. We can therefore take the same course of action to find a uniform approximation that has the above two limits: (i) evaluate the asymptotic amplitudes for large values of x (i.e., for large ϵ), (ii) map the exact action shift δS onto the form obtained from perturbation considerations (but with freely adjustable parameters), (iii) include under the integral a parameterized expression of the same form for the product of the amplitude function A and the Jacobian \mathcal{J} of the mapping function, and (iv) adjust all the parameters such that in the asymptotic limit of large

x the correct Gutzwiller amplitudes and actions of the isolated orbits are obtained, while the unperturbed limit (12) is kept for $x = 0$.

This procedure is very similar in spirit to that used by Sieber and Schomerus in their uniform treatment of many types of bifurcations [8]. However, instead of starting from a phase-space representation of the trace formula and expanding the action in normal forms, we use the group integral representation of the (unperturbed) trace formula developed by Creagh and Littlejohn [6]. The latter exploits directly the properties of the symmetry group characteristic of the system H_0 ; it has been used as a starting point for the perturbative trace formula of Creagh [14], as shown above in Eqs. (14,15).

Different from the U(1) case (with the exceptions mentioned at the end of the previous section), the explicit results which we obtain here do depend on the explicit form of the Hamiltonian H_1 . On the other hand, one of the results (that for the standard Hénon-Heiles potential) turns out to apply also to a three-dimensional cavity with small axially-symmetric quadrupole deformations. This is due to the close relation between the SU(2) and the SO(3) symmetry that is broken in the latter case. We will discuss this system in section IV.

3.1 The quartic Hénon-Heiles potential

We first investigate the quartic Hénon-Heiles (HH4) potential in two dimensions, given in polar coordinates by

$$V(r, \theta) = \frac{1}{2} \omega^2 r^2 - \frac{\alpha}{4} r^4 \cos(4\theta), \quad (16)$$

which has recently been investigated [18] in the framework of the semiclassical perturbation theory described above. The limit $\alpha = 0$ is a harmonic oscillator with the SU(2) symmetry. The anharmonic term makes the system non-integrable with mixed classical dynamics. It retains a discrete four-fold rotational symmetry with four saddle-points at the energy $E^* = \omega^4/4\alpha$, through which the particle can escape. The shortest periodic orbits in this system are two pairs of straight-line librating orbits (named A₁ and A₂ in Ref. [18]) and a circulating orbit (named C). Like in the standard cubic Hénon-Heiles (HH) potential [18, 27, 28], the system is scaled with α and its dynamics can be described in terms of one continuous parameter, the scaled energy e defined by

$$e = E/E^* = 4\alpha E/\omega^4. \quad (17)$$

The actions of the periodic orbits are changed in first order of the perturbation by a shift

$$\delta S_1 = \hbar x (\sin^2 \beta \cos^2 \gamma - \cos^2 \beta), \quad \hbar x = S_0 \frac{3}{32} e. \quad (18)$$

Then, the perturbative modulation factor $\mathcal{M}(x)$ in (15) becomes (with $u = \cos \beta$)

$$\mathcal{M}(x) = \frac{1}{4\pi} \int_0^{2\pi} d\gamma \int_0^\pi \sin \beta d\beta e^{ix(\sin^2 \beta \cos^2 \gamma - \cos^2 \beta)} = \frac{1}{2\pi} \int_0^{2\pi} d\gamma \int_0^1 du e^{ix[(1-u^2)\cos^2 \gamma - u^2]}. \quad (19)$$

An alternative expression of this is obtained by rotating the unit sphere about an angle $\pi/4$ along the 2 axis:

$$\mathbf{e}'_1 = \frac{1}{\sqrt{2}} \mathbf{e}_1 - \frac{1}{\sqrt{2}} \mathbf{e}_3, \quad \mathbf{e}'_2 = \mathbf{e}_2, \quad \mathbf{e}'_3 = \frac{1}{\sqrt{2}} \mathbf{e}_1 + \frac{1}{\sqrt{2}} \mathbf{e}_3, \quad (20)$$

which leads to

$$\mathcal{M}(x) = \frac{1}{4\pi} \int_0^{2\pi} d\gamma \int_0^\pi \sin \beta d\beta e^{ix \sin(2\beta) \cos \gamma}. \quad (21)$$

This integral can be performed analytically (see [18]) and yields

$$\mathcal{M}(x) = \frac{\pi}{2\sqrt{2}} J_{-1/4} \left(\frac{x}{2} \right) J_{1/4} \left(\frac{x}{2} \right). \quad (22)$$

The asymptotic expansion of the Bessel functions $J_\mu(x)$ for large x leads to three terms which we label according to the names of the periodic orbits:

$$\mathcal{M}(x) \sim \mathcal{M}_C(x) + \mathcal{M}_{A_1}(x) + \mathcal{M}_{A_2}(x), \quad (x \gg 1) \quad (23)$$

with

$$\begin{aligned} \mathcal{M}_C(x) &= \frac{1}{2x} & \Rightarrow & A_C \sim \frac{A_0}{2x}, \\ \mathcal{M}_{A_1}(x) &= \frac{1}{2\sqrt{2}x} \cos(+x - \pi/2) & \Rightarrow & A_{A_1} \sim \frac{A_0}{2\sqrt{2}x}, \\ \mathcal{M}_{A_2}(x) &= \frac{1}{2\sqrt{2}x} \cos(-x + \pi/2) & \Rightarrow & A_{A_2} \sim \frac{A_0}{2\sqrt{2}x}. \end{aligned} \quad (24)$$

The first term corresponds to the loop orbit C, the second and third terms to straight-line libration orbits A_1 and A_2 , respectively; each of them has a discrete degeneracy of two which is included in the amplitudes. These are [18] the only periodic orbits with periods of order $T_0 = 2\pi/\omega$ up to energies $e \lesssim 0.85$. The forms on the left-hand side of Eq. (24) contain the exact Maslov indices $\sigma_C = 0$, $\sigma_{A_1} = +1$, and $\sigma_{A_2} = -1$ of the isolated orbits and, with Eq. (12), yield the asymptotic amplitudes of the trace formula shown on the right-hand side of Eq. (24). For small x , these amplitudes have been shown in Ref. [18] to reproduce numerically well the diverging Gutzwiller amplitudes of the isolated periodic orbits. Note that the action shifts predicted at the first order of the perturbation theory are zero for the orbit C and $\pm \hbar x$ for the orbits A_1 and A_2 , respectively. This can be checked numerically for all orbits, as well as analytically for the orbits A_1 and A_2 . The actions of the latter, being straight-line one-dimensional integrals, can be expressed analytically in terms of complete elliptic integrals (see the appendix) and then be Taylor expanded in powers of e . The result is

$$\begin{aligned} S_{A_1} &= S_0 \left(1 + \frac{3}{32}e + \frac{35}{1024}e^2 + \frac{1155}{65536}e^3 + \dots \right), \\ S_{A_2} &= S_0 \left(1 - \frac{3}{32}e + \frac{35}{1024}e^2 - \frac{1155}{65536}e^3 + \dots \right), \end{aligned} \quad (25)$$

which confirms the first-order action shifts $\pm \hbar x$ given in Eqs. (18,24).

For the following, it is important to trace back the asymptotic forms (24) to singular points of the integral (19). For this, we first evaluate the asymptotic form of the u integral. The stationary point at $u = 0$ yields a term $\sim 1/\sqrt{x}$, and the end point at $u = 1$ yields a term $\sim 1/x$. The latter, after an exact integration over γ , gives the contribution $\mathcal{M}_{A_2}(x)$. The γ integral over the first term has four stationary points; saddle-point integration at $\gamma = 0$ and π

yields the contribution $\mathcal{M}_{A_1}(x)$, and at $\gamma = \pi/2$ and $3\pi/2$ it yields the contribution $\mathcal{M}_C(x)$. In summary, we get the periodic orbit contributions asymptotically as follows:

$$\begin{aligned} \text{orbit } A_2 : & \quad \text{from } u = 1, \quad (\text{any } \gamma), \\ \text{orbit } A_1 : & \quad \text{from } u = 0, \quad \gamma = 0 \text{ and } \pi, \\ \text{orbit } C : & \quad \text{from } u = 0, \quad \gamma = \pi/2 \text{ and } 3\pi/2. \end{aligned} \quad (26)$$

We now construct a uniform approximation which for large x yields the correct asymptotic Gutzwiller trace formula with the contributions from the three leading isolated orbits A_1 , A_2 , and C . For describing the gross-shell structure of the level density, it is sufficient to include only the lowest few harmonics,* i.e., the first few repetitions r of the primitive orbits, in the trace formula. In the following, we shall only give the results for $r = 1$; higher repetitions can be included according to Eq. (14). Hence, the Gutzwiller limit is written as

$$\delta g_G = A_{A_1} \cos\left(\frac{S_{A_1}}{\hbar} - \sigma_{A_1} \frac{\pi}{2}\right) + A_{A_2} \cos\left(\frac{S_{A_2}}{\hbar} - \sigma_{A_2} \frac{\pi}{2}\right) + A_C \cos\left(\frac{S_C}{\hbar} - \sigma_C \frac{\pi}{2}\right), \quad (27)$$

This limit can be imposed by including under the integral (19) the product of amplitude function $A(u, \gamma)$ times Jacobian $\mathcal{J}(u, \gamma)$ in the same form as in the exponent, but with different parameters:

$$\begin{aligned} \mathcal{M}_u(x) = & \frac{1}{2\pi} \int_0^{2\pi} d\gamma \int_0^1 du e^{ix[(1-u^2)\cos^2\gamma - u^2]} \times \\ & \times \frac{2x}{A_0} \left\{ \sqrt{2}A_{A_2}u^2 + (1-u^2) \left[\sqrt{2}A_{A_1}\cos^2\gamma + A_C\sin^2\gamma \right] \right\}. \end{aligned} \quad (28)$$

Note that the coefficients in the second line are precisely the inverses of the asymptotic amplitudes given in (24). In this way, the approximation (28) leads by construction to the Gutzwiller limit (27) for large x , whereas for $x \rightarrow 0$ the diverging Gutzwiller amplitudes exactly cancel altogether and $\mathcal{M}_u \rightarrow 1$, as required.

The integrals occurring in (28) can all be done analytically. For the integral appearing as the coefficient of A_C , we note that $e_2^2 = \sin^2\beta \sin^2\gamma$ is invariant under the rotation (20), so that we can replace the phase in the exponent by that appearing in Eq. (21). Then, using the same transformations as in Ref. [18] for obtaining the form (22) of the perturbative modulation factor, and exploiting some recurrence relations amongst the Bessel functions $J_\mu(x)$, we obtain

$$\begin{aligned} & \frac{1}{2\pi} \int_0^{2\pi} d\gamma \frac{1}{2} \int_0^\pi \sin\beta d\beta \sin^2\beta \sin^2\gamma e^{ix \sin(2\beta) \cos\gamma} \\ & = \frac{\pi}{4\sqrt{2}} \left[J_{-1/4}\left(\frac{x}{2}\right) J_{1/4}\left(\frac{x}{2}\right) - J_{-3/4}\left(\frac{x}{2}\right) J_{3/4}\left(\frac{x}{2}\right) \right]. \end{aligned} \quad (29)$$

The other two integrals can be found first by taking the derivative of Eq. (19) with respect to x , and second by integrating the terms proportional to u^2 in (28) over u by parts, and finally by

*A more consistent truncation of the trace formula, followed below, is achieved by Gaussian smoothing over a small energy range γ , resulting in the amplitudes multiplied by exponential damping factors; see Ref. [28] for details. These exponential factors are included in the amplitudes A_{A_1} , A_{A_2} , and A_C and their combinations defined below.

taking suitable linear combinations of the results of these two operations. The final expression is

$$\mathcal{M}_u(x) = \frac{2x}{A_0} \left[A_C \mathcal{M}_-(x) + \sqrt{2} \bar{A}_A \mathcal{M}_+(x) - i\sqrt{2} \Delta A_A \mathcal{M}'(x) \right], \quad (30)$$

where

$$\bar{A}_A = \left(\frac{A_{A_1} + A_{A_2}}{2} \right), \quad \Delta A_A = \left(\frac{A_{A_1} - A_{A_2}}{2} \right), \quad (31)$$

and

$$\begin{aligned} \mathcal{M}_\pm(x) &= \frac{\pi}{4\sqrt{2}} \left[J_{-1/4}\left(\frac{x}{2}\right) J_{1/4}\left(\frac{x}{2}\right) \pm J_{-3/4}\left(\frac{x}{2}\right) J_{3/4}\left(\frac{x}{2}\right) \right], \\ \mathcal{M}'(x) &= -\frac{\pi}{4\sqrt{2}} \left[J_{-1/4}\left(\frac{x}{2}\right) J_{5/4}\left(\frac{x}{2}\right) + J_{1/4}\left(\frac{x}{2}\right) J_{3/4}\left(\frac{x}{2}\right) \right]. \end{aligned} \quad (32)$$

The last step now is to insert the modulation factor (30) into Eq. (14) and to replace the unperturbed action S_0 in the phase of the first term of (30) by S_C , and for the other two terms by the average action \bar{S}_A of the orbits S_{A_1} and S_{A_2} , while the perturbative action shift $\hbar x$ is redefined as their difference ΔS_A

$$\hbar x = \Delta S_A = \frac{1}{2} (S_{A_1} - S_{A_2}), \quad \bar{S}_A = \frac{1}{2} (S_{A_1} + S_{A_2}). \quad (33)$$

By these replacements, we ensure that the phases in the asymptotic level density (27) contain the correct numerical actions of the isolated orbits.

The final form of the uniform level density for the HH4 potential (including only the primitive orbits, i.e., $r = 1$) is then:

$$\begin{aligned} \delta g_u &= (2\Delta S_A/\hbar) \Re \left\{ e^{\frac{i}{\hbar} S_C} A_C \mathcal{M}_-(\Delta S_A/\hbar) \right. \\ &\quad \left. + \sqrt{2} e^{\frac{i}{\hbar} \bar{S}_A} \left[\bar{A}_A \mathcal{M}_+(\Delta S_A/\hbar) - i \Delta A_A \mathcal{M}'(\Delta S_A/\hbar) \right] \right\} \\ &= (2\Delta S_A/\hbar) \left\{ A_C \mathcal{M}_-(\Delta S_A/\hbar) \cos(S_C/\hbar) \right. \\ &\quad \left. + \sqrt{2} \left[\bar{A}_A \mathcal{M}_+(\Delta S_A/\hbar) \cos(\bar{S}_A/\hbar) + \Delta A_A \mathcal{M}'(\Delta S_A/\hbar) \sin(\bar{S}_A/\hbar) \right] \right\}. \end{aligned} \quad (34)$$

As in the case of the TGU uniform approximation discussed in Sec. II, this formula only holds as long as no bifurcations of the stable isolated orbits occur. For the primitive orbits of the HH4 system, this does not happen up to $e \simeq 0.85$, where the primitive orbit A_1 undergoes an isochronous bifurcation. In the numerical results shown below, we have smoothed the Gutzwiller amplitude of this orbit (see Ref. [18] for details) in order to simulate a better treatment of this bifurcation by the corresponding uniform approximation [8].

In Fig. 1 we show a numerical compilation of the three semiclassical approximations to the level density δg discussed here (given by dashed lines) and compare them to the quantum-mechanical one (given by the solid lines). In all cases, Gaussian averaging over the energy E with a range $\gamma = 0.6 \hbar \omega$ has been applied. This damps the amplitudes strongly enough so that only the primitive orbits ($r = 1$) need be kept in the semiclassical approaches. At the bottom of this figure, the Gutzwiller result (27) for the isolated orbits is shown. It gives an excellent agreement with the quantum result for $E \gtrsim 10 \hbar \omega$, even up to $e \simeq 1$ (the saddle energy is $E^* \simeq 39 \hbar \omega$ for the case $\alpha = 0.0064$ chosen here). For small energies, it diverges due to the approaching SU(2) symmetry limit. In the middle of the figure, the perturbative

result [18] is shown. It reproduces the quantum result up to $E \sim 13 \hbar\omega$, thus catching the essential feature of the symmetry breaking. (Note that at $E \sim 13 \hbar\omega$ we have $x \sim 3$, showing that the perturbative approach may be used also for values of x somewhat larger than unity, cf. [14, 18].) For $E > 14 \hbar\omega$ the anharmonicity is, however too large for perturbation theory to apply. Finally, the top part of Fig. 1 shows the present uniform approximation that reproduces the quantum result at all energies.

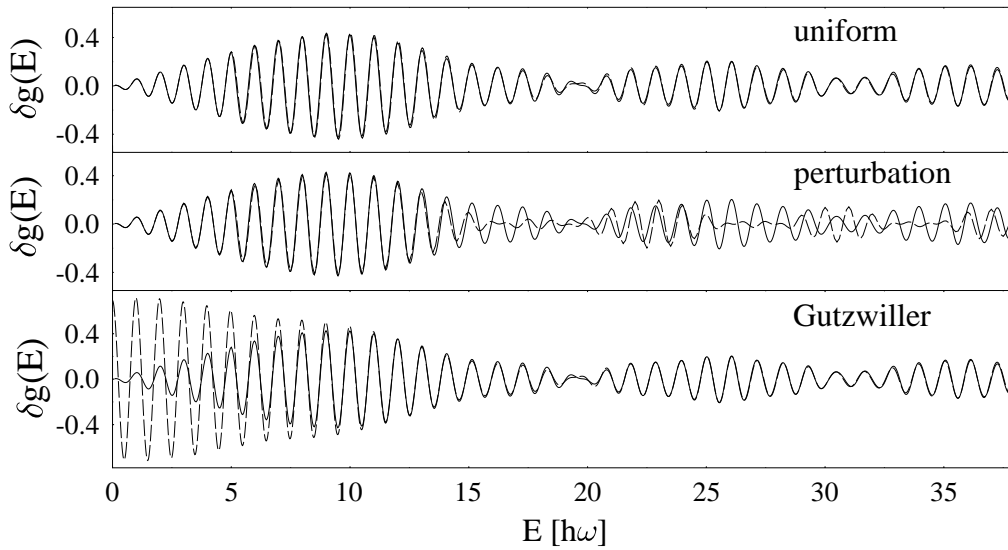


Figure 1: Oscillating part of level density of the HH4 potential ($\alpha = 0.0064$), averaged over a range $\gamma = 0.6$, versus energy E (units: $\hbar\omega$). Solid lines: quantum-mechanical results. Dashed lines: semiclassical approximations (with $r_m = 1$). Bottom: Gutzwiller trace formula (diverging at small energies); middle: perturbative trace formula by Creagh (failing at large energies); top: present uniform approximation (working at all energies).

In Fig. 2 we compare the results of the present uniform approximation (dashed lines) with the quantum results (solid lines) for two different values of the anharmonicity parameter α . In the two upper panels, the same smoothing width $\gamma = 0.6 \hbar\omega$ was used as in the previous figure and only the primitive orbits ($r = 1$) A_1 , A_2 and C were included. In the two lower panels, we have used a smaller smoothing width $\gamma = 0.25 \hbar\omega$ and included the second repetitions (i.e., $r_m = 2$) of the three orbits as well. Now a more detailed fine structure of the level spectrum is resolved; even this is well reproduced by the semiclassical approximation. Only in the regions corresponding to $e = E/E^* \gtrsim 0.8$ ($E \gtrsim 31 \hbar\omega$), some small differences can be seen which are explained by the fact that at these energies, new orbits with actions comparable to those of the included orbits with $r = 2$ exist (after period-doubling bifurcations of the orbits C and A_1) which we have not included. Their inclusion would necessitate a proper uniform treatment of the corresponding bifurcations, which is outside the scope of this paper.

In the actual computation of the uniform trace formula for small energies e , cancellations between the diverging Gutzwiller amplitudes take place. This requires their rather accurate numerical determination. For practical purposes, it is advisable to take advantage of the fact that for sufficiently small arguments $x = \Delta S_A/\hbar$, the result (34) goes over into the perturbative trace formula (14) with the modulation factor (22) which is numerically much more robust. We

found that one may switch between the two formulae for values $1.5 \lesssim x \lesssim 2.5$ without visibly changing the results shown above.

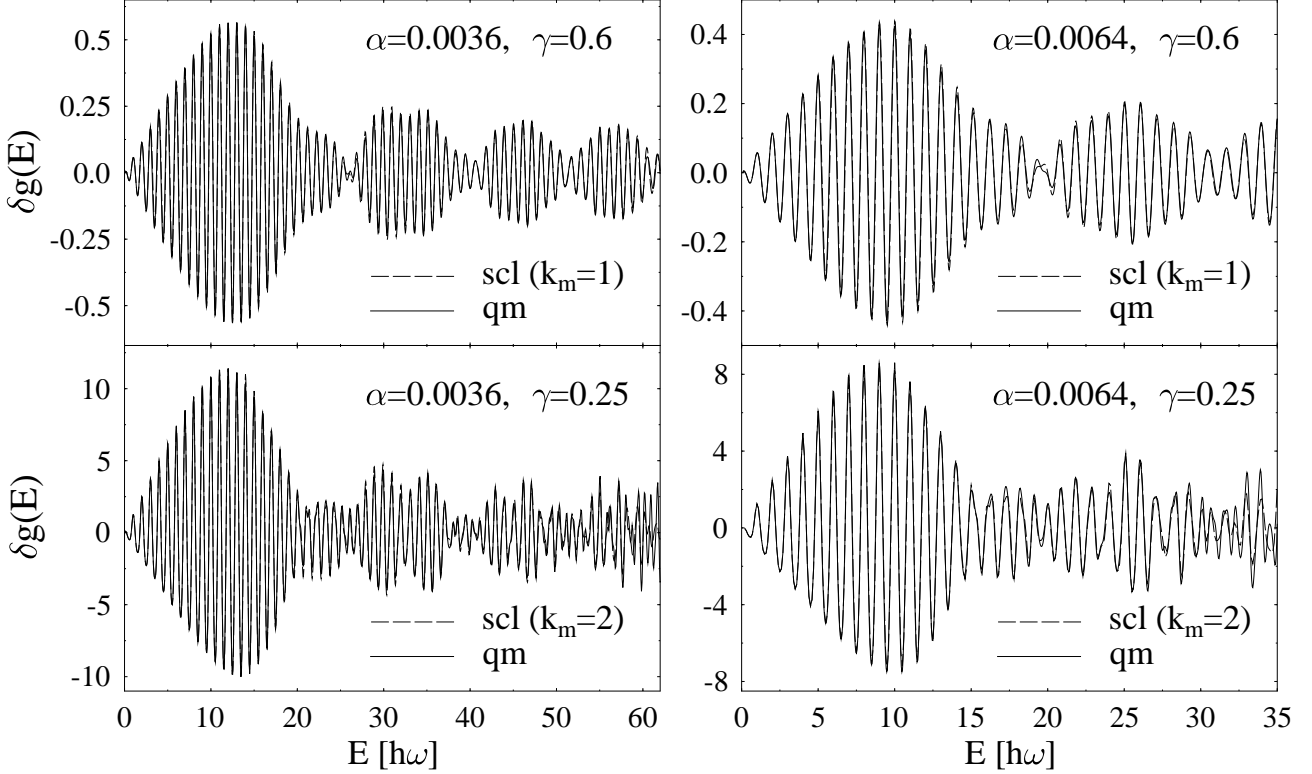


Figure 2: Oscillating part of level density of the HH4 potential versus energy E (units: $\hbar\omega$). Solid lines: quantum-mechanical results. Dashed lines: semiclassical results with present uniform approximation. Left side: $\alpha = 0.0036$ ($E^* \simeq 69 \hbar\omega$), right side: $\alpha = 0.0064$ ($E^* \simeq 39 \hbar\omega$). Upper part: $\gamma = 0.6$ and $r_m = 1$, lower part: $\gamma = 0.25$ and $r_m = 2$.

3.2 The standard Hénon-Heiles potential

We will now investigate the original Hénon-Heiles (HH) potential [27], given in polar coordinates by

$$V(r, \theta) = \frac{1}{2} \omega^2 r^2 - \frac{\alpha}{3} r^3 \cos(3\theta). \quad (35)$$

The three shortest isolated orbits in this potential, which have been shown [28] to govern the beating gross-shell structure in the level density of this system, are a straight-line librating orbit A, a curved librating orbit B, and a circulating orbit C (similar to that in the HH4 potential). Orbits A and B have a discrete degeneracy of three, due to the three-fold discrete rotational symmetry of the potential (35), and the orbit C is two-fold degenerate due to time reversal symmetry.

Because of the odd power of the anharmonic term in (35), the first-order perturbation result is zero both classically and quantum-mechanically. In second-order perturbation, the action shift δS due to the anharmonicity is given [18] by

$$\delta S_2 = \hbar x (5 - 7 \cos^2 \beta) / 6, \quad (36)$$

with

$$\hbar x = \frac{S_0}{12} \frac{E}{E^*} = \frac{S_0}{12} e, \quad E^* = \frac{\omega^6}{6\alpha^2}. \quad (37)$$

Here E^* is the saddle energy for the potential (35), and S_0 is the action of the unperturbed harmonic oscillator given in (12). The perturbative modulation factor $\mathcal{M}(x)$ becomes

$$\mathcal{M}(x) = \frac{1}{4\pi} \int d\Omega e^{ix(5-7u^2)/6} = \int_0^1 du e^{ix(5-7u^2)/6}. \quad (38)$$

This integral can be expressed analytically in terms of the Fresnel functions $C(x)$ and $S(x)$ (we use the convention of Abramowitz and Stegun [29]):

$$\mathcal{M}(x) = e^{5ix/6} \frac{1}{\xi} [C(\xi) - iS(\xi)], \quad \xi = \sqrt{\frac{7|x|}{3\pi}}. \quad (39)$$

Using the asymptotic expansion of the Fresnel functions for large arguments $x \gg 1$,

$$\begin{aligned} C(\xi) &\sim \frac{1}{2} + \frac{1}{\pi\xi} \sin(\pi\xi^2/2), \\ S(\xi) &\sim \frac{1}{2} - \frac{1}{\pi\xi} \cos(\pi\xi^2/2), \end{aligned} \quad (40)$$

we get the asymptotic result

$$\delta g \sim \sqrt{\frac{3\pi}{14|x|}} A_0 \cos(S_0/\hbar + 5x/6 - \pi/4) + \frac{3}{7|x|} A_0 \cos(S_0/\hbar - x/3 + \pi/2), \quad (41)$$

which is again only correct for sufficiently small values of the scaled energy e so that $x \lesssim 1$. Note that (41) predicts the action shift ΔS_C and the average action shift ΔS_{AB} to be

$$\Delta S_C = S_C - S_0 = -\hbar x/3, \quad \Delta S_{AB} = \bar{S}_{AB} - S_0 = 5\hbar x/6, \quad \bar{S}_{AB} = \frac{1}{2}(S_A + S_B). \quad (42)$$

This is numerically well fulfilled at lower energies. The expansion (41) is also obtained from the asymptotic analysis of the integral (38), whereby the first term comes from the stationary point at $u = 0$ and the second term is the end-point correction from $u = 1$. The latter corresponds to the C orbit in the HH potential with the correct Maslov index [18] $\sigma_C = -1$. Its amplitude is thus predicted in the second-order perturbation theory as

$$A_C^{pt2} = \frac{6E}{7(\hbar\omega)^2 x} = \frac{36}{7\pi\hbar\omega} \frac{1}{e}, \quad (43)$$

which was shown in Ref. [18] to describe well the numerical Gutzwiller amplitude A_C , not only for small e where it diverges, but also up to energies $e \simeq 1$. The first term in (41) corresponds to the sum of orbits A and B which, however, are still degenerate on the circle $\gamma \in [0, 2\pi)$ at the second order of the perturbation expansion and therefore have an asymptotic amplitude too large by a factor $1/\sqrt{\hbar}$. These orbits are broken up only at fourth order, with an action shift

$$\delta S_4 = -\hbar y \sin^3 \beta \cos(3\gamma), \quad y = c_4 e^3. \quad (44)$$

Including this into the phase of the modulation factor, we get

$$\begin{aligned}\mathcal{M}(x, y) &= \int_0^1 du e^{ix(5-7u^2)/6} \frac{1}{2\pi} \int_0^{2\pi} d\gamma e^{-iy(1-u^2)^{3/2} \cos(3\gamma)} \\ &= \int_0^1 du e^{ix(5-7u^2)/6} J_0[y(1-u^2)^{3/2}].\end{aligned}\quad (45)$$

In the asymptotic expansion of this modulation factor, the Bessel function modifies only the contribution from the stationary point at $u = 0$, leading to

$$\delta g \sim \sqrt{\frac{3\pi}{14|x|}} A_0 J_0(y) \cos(S_0/\hbar + 5x/6 - \pi/4) + \frac{3}{7|x|} A_0 \cos(S_0/\hbar - x/3 + \pi/2). \quad (46)$$

Upon further expansion of $J_0(y)$ for $y \gg 1$, this yields the amplitudes and the correct Maslov phases [18] $\sigma_A = 1$ and $\sigma_B = 0$ of the (now isolated) orbits A and B. The amplitudes, which are equal at this order of the perturbation theory, go like $1/\sqrt{|xy|}$ and thus have the same power of \hbar as A_C^{pt2} . The actions of the orbits A and B are shifted from the average value \bar{S}_{AB} by an amount $\pm \hbar y$, respectively. For the orbit A, this can again be checked by analytical integration (see the appendix) and Taylor expansion of its period. The action becomes

$$S_A = S_0 \left(1 + \frac{5}{72}e + \frac{385}{15552}e^2 + \frac{85085}{6718464}e^3 + \dots \right). \quad (47)$$

The first correction term is the average action shift ΔS_{AB} (42), obtained for both orbits A and B at second order of the perturbation theory; the next term gives the value of c_4 in Eq. (44). With this, the fourth-order prediction of the average amplitude of orbits A and B becomes

$$A_{AB}^{pt4} = \frac{E}{(\hbar\omega)^2} \sqrt{\frac{3}{7|xy|}} = \frac{216}{7\pi\hbar\omega} \sqrt{\frac{3}{55}} \frac{1}{e^{3/2}}. \quad (48)$$

[Note that this amplitude contains the degeneracy factor 3 of the orbits A and B mentioned above; it is related to the factor 3 in the argument of the cos function in (44). Similarly, A_C^{pt2} (43) contains the time-reversal factor 2 of the orbit C, which is related to the two end-point corrections, coming from the u integral in (38) which originally runs from -1 to $+1$, each giving one half of the second term in (41).]

We now redefine the quantities x and y in terms of the true actions of the isolated periodic orbits

$$\hbar y = \delta S = \frac{1}{2}(S_A - S_B), \quad \frac{7}{6}\hbar x = \Delta S = \frac{1}{2}(S_A + S_B) - S_C, \quad (49)$$

and introduce the combinations of the Gutzwiller amplitudes

$$\bar{A}_{AB} = \frac{1}{2}(A_A + A_B), \quad \Delta A_{AB} = \frac{1}{2}(A_A - A_B). \quad (50)$$

The uniform approximation to the modulation factor is then

$$\begin{aligned}\mathcal{M}_u &= \frac{1}{A_0} \int_0^1 du e^{(i/\hbar) \Delta S (5/7 - u^2)} \frac{1}{2\pi} \int_0^{2\pi} d\gamma e^{-(i/\hbar) \delta S (1-u^2)^{3/2} \cos(3\gamma)} \times \\ &\times \left\{ \frac{2|\Delta S|}{\hbar} A_C u^2 + \sqrt{\frac{4|\Delta S|}{\hbar\pi}} (1-u^2) \sqrt{\frac{2\pi|\delta S|}{\hbar}} [\bar{A}_{AB} + \Delta A_{AB} \cos(3\gamma)] \right\}. \quad (51)\end{aligned}$$

The second line above is again the parameterized product $A(u, \gamma) \mathcal{J}(u, \gamma)$, with coefficients chosen such that asymptotically for large ΔS and δS , the Gutzwiller limit

$$\delta g_G = A_A \cos(S_A/\hbar - \sigma_A \pi/2) + A_B \cos(S_B/\hbar - \sigma_B \pi/2) + A_C \cos(S_C/\hbar - \sigma_C \pi/2) \quad (52)$$

is reached. (The degeneracy factors due to discrete symmetries discussed above are again included in the amplitudes.) In the limit $\Delta S = \delta S = 0$, on the other hand, \mathcal{M}_u (51) still reduces to unity as it should.

The two-dimensional integrals in (51) cannot be done analytically here. It turns out, however, that we can approximate them without violating the above two limits.[†] For that we note that the first term (corresponding to orbit C) asymptotically gets contributions only from $u \simeq 1$; we may therefore put $u = 1$ in the exponent of the γ integral which then becomes unity. The second term of (51), corresponding to the orbits A and B, asymptotically only gets contributions from $u \simeq 0$. Putting $u = 0$ in the exponents of the γ integrals leads to Bessel functions J_0 and J_1 like in the TGU formula (11). The remaining u integrals can now be expressed again in terms of the Fresnel functions after some partial integrations; hereby we keep only the leading-order terms in \hbar . We then arrive at the uniform trace formula for the HH potential, including the contributions from the three primitive orbits A, B, and C,

$$\begin{aligned} \delta g_u = & A_C \cos\left(\frac{S_C}{\hbar} + \frac{\pi}{2}\right) \\ & - \sqrt{\left|\frac{2\delta S}{\Delta S}\right|} \left[\bar{A}_{AB} J_0\left(\frac{\delta S}{\hbar}\right) \cos\left(\frac{S_C}{\hbar} + \frac{\pi}{2}\right) - \Delta A_{AB} J_1\left(\frac{\delta S}{\hbar}\right) \sin\left(\frac{S_C}{\hbar} + \frac{\pi}{2}\right) \right] \\ & + C \left(\sqrt{\frac{2|\Delta S|}{\hbar\pi}} \right) \sqrt{\frac{4\pi|\delta S|}{\hbar}} \left[\bar{A}_{AB} J_0\left(\frac{\delta S}{\hbar}\right) \cos\left(\frac{\bar{S}_{AB}}{\hbar}\right) - \Delta A_{AB} J_1\left(\frac{\delta S}{\hbar}\right) \sin\left(\frac{\bar{S}_{AB}}{\hbar}\right) \right] \\ & + S \left(\sqrt{\frac{2|\Delta S|}{\hbar\pi}} \right) \sqrt{\frac{4\pi|\delta S|}{\hbar}} \left[\bar{A}_{AB} J_0\left(\frac{\delta S}{\hbar}\right) \sin\left(\frac{\bar{S}_{AB}}{\hbar}\right) + \Delta A_{AB} J_1\left(\frac{\delta S}{\hbar}\right) \cos\left(\frac{\bar{S}_{AB}}{\hbar}\right) \right] \quad (53) \end{aligned}$$

In the low-energy limit $\Delta S \rightarrow 0$, $\delta S \rightarrow 0$, the second line of (53) cancels the orbit C term in the first line, the fourth line vanishes, and the third line yields the HO trace formula (12).

At energies where the C orbit is well isolated and separated from the A and B orbits ($\Delta S \gg \hbar$) but the splitting of A and B is still small ($\delta S \lesssim \hbar$), we can use the asymptotic forms (40) of the Fresnel functions. Hereby the second terms from (40) combine to cancel the second line in (53), whereas the leading terms combine into

$$\begin{aligned} \delta g_u = & A_C \cos\left(\frac{S_C}{\hbar} + \frac{\pi}{2}\right) + \sqrt{\frac{2\pi|\delta S|}{\hbar}} \times \\ & \times \left[\bar{A}_{AB} J_0\left(\frac{\delta S}{\hbar}\right) \cos\left(\frac{\bar{S}_{AB}}{\hbar} - \frac{\pi}{4}\right) - \Delta A_{AB} J_1\left(\frac{\delta S}{\hbar}\right) \sin\left(\frac{\bar{S}_{AB}}{\hbar} - \frac{\pi}{4}\right) \right], \quad (x \gg 1) \quad (54) \end{aligned}$$

so that the second line contains nothing but the TGU approach to orbits A and B, kept separate from the isolated orbit C contribution.

[†]These approximations correspond, in fact, to neglecting only higher-order terms in \hbar . We have checked by numerical integration that these do not affect the results discussed below.

In Fig. 3 we show the numerical results obtained with the uniform approximation (53) using $r_m = 2$ (dashed line), compared with the quantum-mechanical result (solid line) for the HH potential with $\alpha = 0.04$ and a Gaussian averaging with width $\gamma = 0.25 \hbar\omega$. The agreement is perfect for all energies up to $e \sim 0.73$. The differences seen for $e \gtrsim 0.73$ are due to some missing orbits which arise after period-doubling bifurcations of the primitive orbits A and C, and perhaps to the isochronous bifurcation of the A orbit that occurs only at $e \simeq 0.97$ but may make itself felt in the amplitude A_A already at smaller energies. (Note that, in contrast to the HH4 case above, we have not smoothed this amplitude here.) All these bifurcations can be treated with the uniform approximations developed in Refs. [8]. Part of the disagreement for $e \gtrsim 0.75$ is also due to inaccuracies in the diagonalisation of the quantum HH Hamiltonian in a finite basis [28].

Like in the case of the HH4 potential, the SU(2) limit is reached in the uniform approximation (53) through a subtle cancellation of divergences in the Gutzwiller amplitudes. Numerically, the most robust procedure is to use the perturbative result (39) for values of $x = 6\Delta S/7\hbar$ up to $\sim 1.5 - 2.5$, and then to switch to the uniform approximation.

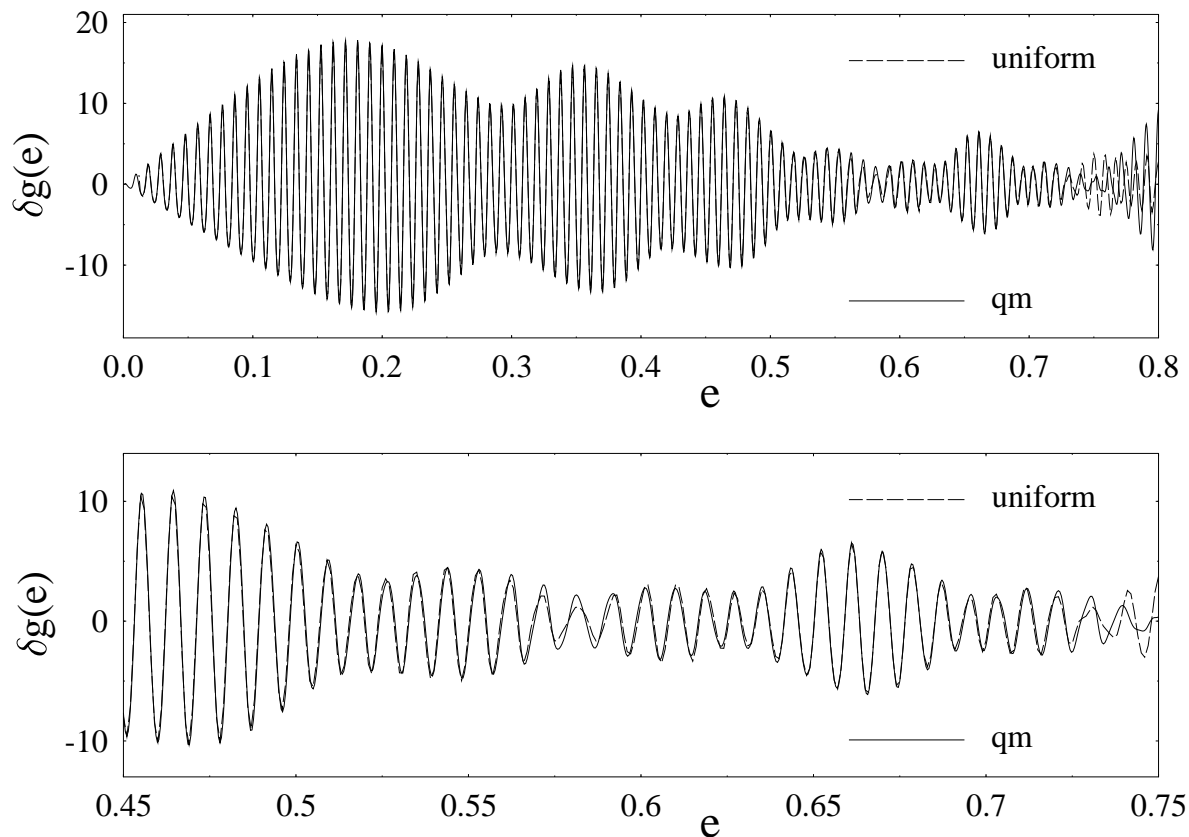


Figure 3: Oscillating part of level density of the Hénon-Heiles potential ($\alpha = 0.04$), Gaussian averaged over a range $\gamma = 0.25$, versus scaled energy e . Solid line: quantum-mechanical result; dashed line: semiclassical result in the present uniform approximation with $r_m = 2$. (Units: $\hbar\omega$.)

4 Axial quadrupole deformations of a spherical cavity

We finally discuss three-dimensional cavities with axially symmetric quadrupole deformations that can be treated with the uniform approximation developed above for the HH potential. The boundary of the cavities is in polar coordinates given by

$$R(\theta, \phi) = R_0 [1 + \epsilon P_2(\cos \theta)], \quad (55)$$

where $P_2(x) = (3x^2 - 1)/2$ is the second Legendre polynomial. The periodic orbits in a spherical cavity with ideally reflecting walls have been discussed extensively by Balian and Bloch [2], and an analytical trace formula has been given by these authors for its level density which we again write as in Eq. (4). The three-dimensional degeneracy of the polygonal orbits with $N \geq 3$ corners, due to the $SO(3)$ symmetry of the sphere, can be described by the three Euler angles (α, β, γ) , and the corresponding group integral is [6, 14]

$$\frac{1}{8\pi^2} \int_0^{2\pi} d\gamma \int_0^\pi \sin \beta d\beta \int_0^{2\pi} d\alpha = 1. \quad (56)$$

We choose the Euler angles such that β is the angle between the normal to the plane of motion of an orbit family and the z axis, γ describes the orientation of a single orbit within this plane (i.e., within the family), and α describes rotations of the orbit plane around the z axis. As long as we restrict the deformations of the cavity to be axially symmetric (around the z axis), the action of the perturbed orbits will not depend on the angle α . For small deformations, the contribution of each periodic orbit family to the spherical trace formula can thus again be written in the perturbative approach as

$$\delta g_{pert} = \Re e \left\{ \mathcal{M}(x, y) e^{i(S_0/\hbar - \sigma_0 \pi/2)} \right\}, \quad (57)$$

where the modulation factor is

$$\mathcal{M}(x, y) = \frac{1}{2\pi} \int_0^{2\pi} d\gamma \int_0^1 du e^{i\delta S(u, \gamma; x, y)}. \quad (58)$$

Here x and y are parameters depending on the deformation ϵ , the energy, and the specific orbit type. When both x and y are non-zero, the orbit families are broken into singly degenerate families of orbits lying in planes. These come in two types. One type is lying in planes perpendicular to the symmetry axis (coming from the end-point correction at $u = 1$); we will henceforth call them the *equatorial orbits*. They are identical to the orbits in a two-dimensional circular billiard. The other type of orbits lie in planes that contain the symmetry axis (coming from the stationary point $u = 0$); we will call these the *planar orbits*. They are isolated in their plane of motion and will, for small deformations, come in pairs of stable and unstable orbits. With the exception of a completely isolated linear orbit that oscillates along the symmetry axis, all the equatorial and planar orbits have the continuous one-parameter degeneracy due to rotation of the plane of motion around the symmetry axis.

We see therefore that the situation is completely analogous to that of the HH potential discussed in the previous section: orbit C corresponds to the equatorial orbit families (with two orientations connected to time reversal), and the orbits A and B to the pairs of planar orbits. The only difference is that, since we start here from a three-dimensional system with $SO(3)$

symmetry, the breaking of two degrees of degeneracy leaves the orbits in singly degenerate families. Furthermore, the planar orbits do not have the discrete three-fold rotational degeneracy as the A and B orbits in the HH potential, but occasional two-fold degeneracies due to the symmetry of reflection at the equator plane. We can therefore take over the previous results with little effort. We shall first discuss the family of polygon orbits with $N \geq 3$ corners, and come to the diameter orbits ($N = 2$) later.

4.1 Polygon orbits with $N \geq 3$

The families of polygon orbits in the sphere have in principle the full $\text{SO}(3)$ symmetry. However, when we limit the deformation of the cavity to axially-symmetric shapes, the action shift depends only on two of the Euler angles, so that the symmetry breaking problem is the same as in the HH potential considered above. In first-order perturbation theory [15], the action shift depends only on the angle β :

$$\delta S_1 = -\Delta S P_2(\cos \beta), \quad \Delta S = \frac{\epsilon}{2} S_0. \quad (59)$$

This corresponds to the fact that a quadrupole deformation to lowest order in ϵ is identical to that of an axially symmetric ellipsoid, which is an integrable system and thus has an extra symmetry with two-fold degenerate orbit families (i.e., polygons with $N \geq 3$ fitting into the ellipse that gives the boundary of the plane of motion). As for the orbits A and B of the HH system, this symmetry will be broken only at a higher order in the perturbation expansion; in the present case we expect this to happen at the third order in ϵ , with an action shift

$$\delta S_3 = -\delta S_{pl} \sin^3 \beta \cos(n\gamma), \quad (60)$$

where n counts the discrete symmetries of the planar orbits and will again be absorbed into the Gutzwiller amplitudes. With this, the modulation factor becomes

$$\mathcal{M}(x, y) = \int_0^1 du e^{ix(1-3u^2)/2} \frac{1}{2\pi} \int_0^{2\pi} d\gamma e^{-iy(1-u^2)^{3/2} \cos(n\gamma)} \quad (61)$$

with $\hbar x = \Delta S$ and $\hbar y = \delta S_{pl}$. For small x and y , the action shifts will be

$$\begin{aligned} (u = 1) : \quad & S_{eq} - S_0 = -x = -\hbar \Delta S, \\ (u = 0) : \quad & \bar{S}_{pl} - S_0 = +x/2 = +\hbar \Delta S/2, \end{aligned} \quad (62)$$

with

$$\bar{S}_{pl} = \frac{1}{2}(S_{pl}^u + S_{pl}^s), \quad S_{pl}^u = \bar{S}_{pl} + \delta S_{pl}, \quad S_{pl}^s = \bar{S}_{pl} - \delta S_{pl}. \quad (63)$$

The modulation factor (61) has exactly the same form as that of the HH case (45). However, different from there, x and y can have both signs, depending on the sign of ϵ . Therefore, switching from prolate deformations ($\epsilon > 0$), which is analogous to the HH situation, to oblate deformations ($\epsilon < 0$), one has to take the complex conjugate of the modulation factor before using it in (57). This only affects some of the signs in the final results; in the following formulae the upper signs correspond to the prolate case and the lower signs to the oblate case.

The final trace formula for one type of orbits (with fixed number $N \geq 3$ of corners, and without including their higher repetitions) becomes

$$\begin{aligned} \delta g_u^{(N \geq 3)} &= A_{eq} \cos \Phi_{eq} - \sqrt{\frac{2|\delta S|}{|\Delta S|}} \left[\bar{A}_{pl} J_0\left(\frac{\delta S}{\hbar}\right) \cos \Phi_{eq} - \Delta A_{pl} J_1\left(\frac{\delta S}{\hbar}\right) \sin \Phi_{eq} \right] \\ &+ C \left(\sqrt{\frac{2|\Delta S|}{\pi \hbar}} \right) \sqrt{\frac{4\pi|\delta S|}{\hbar}} \left[\bar{A}_{pl} J_0\left(\frac{\delta S}{\hbar}\right) \cos \bar{\Phi}_{pl} - \Delta A_{pl} J_1\left(\frac{\delta S}{\hbar}\right) \sin \bar{\Phi}_{pl} \right] \\ &\pm S \left(\sqrt{\frac{2|\Delta S|}{\pi \hbar}} \right) \sqrt{\frac{4\pi|\delta S|}{\hbar}} \left[\bar{A}_{pl} J_0\left(\frac{\delta S}{\hbar}\right) \sin \bar{\Phi}_{pl} + \Delta A_{pl} J_1\left(\frac{\delta S}{\hbar}\right) \cos \bar{\Phi}_{pl} \right], \quad (64) \end{aligned}$$

where we have redefined

$$\begin{aligned} \frac{3}{2}\hbar x &= \Delta S = \bar{S}_{pl} - S_{eq}, & \hbar y &= \delta S = \frac{1}{2}(S_{pl}^u - S_{pl}^s), \\ \Phi_{eq} &= \frac{S_{eq}}{\hbar} - \sigma_{eq} \frac{\pi}{2}, & \bar{\Phi}_{pl} &= \frac{\bar{S}_{pl}}{\hbar} - \sigma_0 \frac{\pi}{2}. \end{aligned} \quad (65)$$

and the combinations of Gutzwiller amplitudes (including discrete degeneracy factors)

$$\bar{A}_{pl} = \frac{1}{2}(A_{pl}^u + A_{pl}^s), \quad \Delta A_{pl} = \frac{1}{2}(A_{pl}^u - A_{pl}^s). \quad (66)$$

The correct Maslov indices of the asymptotic orbits become

$$\sigma_{eq} = \sigma_0 \mp 1, \quad \bar{\sigma}_{pl} = \frac{1}{2}(\sigma_{pl}^u + \sigma_{pl}^s) = \sigma_0 \pm \frac{1}{2}, \quad \sigma_{pl}^u = \sigma_{pl}^s + 1. \quad (67)$$

At moderately large deformations, the equatorial and planar orbits are sufficiently well separated, so that we can take the limit $|\delta S| \gg \hbar$. The result (64) then simplifies to

$$\begin{aligned} \delta g_u^{(N \geq 3)} &= A_{eq} \cos \Phi_{eq} \\ &+ \sqrt{\frac{2\pi|\delta S|}{\hbar}} \left[\bar{A}_{pl} J_0\left(\frac{\delta S}{\hbar}\right) \cos\left(\frac{\bar{S}_{pl}}{\hbar} - \bar{\sigma}_{pl} \frac{\pi}{2}\right) - \Delta A_{pl} J_1\left(\frac{\delta S}{\hbar}\right) \sin\left(\frac{\bar{S}_{pl}}{\hbar} - \bar{\sigma}_{pl} \frac{\pi}{2}\right) \right] \end{aligned} \quad (68)$$

which again contains the simple TGU formula applied to the planar orbits. At larger deformations (but still before any bifurcations take place), we expand the above for $|\delta S| \gg \hbar$ and obtain the Gutzwiller limit

$$\delta g_G^{(N \geq 3)} = A_{eq} \cos \Phi_{eq} + A_{pl}^u \cos \Phi_{pl}^u + A_{pl}^s \cos \Phi_{pl}^s. \quad (69)$$

4.2 Diameter orbits ($N = 2$)

The diameter orbits ($N = 2$) in a spherical cavity have only a continuous degeneracy of two, since rotation about themselves does not bring about any new orbit [2]. It is convenient to redefine the Euler angles such that β describes the angle between the diameter orbit and the z axis. In first-order perturbation theory, the action shift of the diameter orbit due to a quadrupole deformation (55) is then given by [15]

$$\delta S_1 = \epsilon S_0 P_2(\cos \beta) \quad (70)$$

Hence the modulation factor for small deformations becomes

$$\mathcal{M}(x) = \int_0^1 du e^{ix(3u^2-1)/2} \quad (71)$$

with $\hbar x = \epsilon S_0$. Asymptotically, we get from $u = 0$ the equator orbits which keep the U(1) degeneracy corresponding to rotation about the z axis, and from the end point $u = 1$ we find the isolated diameter orbit along the z axis. Their action shifts for small x will be

$$S_{eq} - S_0 = -\hbar x/2, \quad S_{iso} - S_0 = +\hbar x \quad (72)$$

The situation thus corresponds exactly to the case for the polygonal orbits, but with $y = 0$ since there is no further splitting of the isolated diameter orbit, and with the roles of prolate and oblate deformations interchanged. The uniform trace formula for the diameter contributions is thus

$$\begin{aligned} \delta g_u^{(N=2)} &= \left(A_{iso} - \sqrt{\frac{\hbar}{\pi|\Delta S|}} A_{eq} \right) \cos \Phi_{iso} \\ &+ \sqrt{2} A_{eq} \left[C \left(\sqrt{\frac{2|\Delta S|}{\pi\hbar}} \right) \cos \left(\frac{S_{eq}}{\hbar} - \sigma_0 \frac{\pi}{2} \right) \mp S \left(\sqrt{\frac{2|\Delta S|}{\pi\hbar}} \right) \sin \left(\frac{S_{eq}}{\hbar} - \sigma_0 \frac{\pi}{2} \right) \right]. \end{aligned} \quad (73)$$

Hereby we have (re)defined

$$\Delta S = S_{iso} - S_{eq}, \quad \Phi_{iso} = \frac{S_{iso}}{\hbar} - \sigma_{iso} \frac{\pi}{2}, \quad \sigma_{iso} = \sigma_0 \pm 1. \quad (74)$$

For $|\Delta S| \gg \hbar$, we get the Gutzwiller limit for the diameter orbits:

$$\delta g_G^{(N=2)} = A_{eq} \cos \Phi_{eq} + A_{iso} \cos \Phi_{iso} \quad (75)$$

with

$$\Phi_{eq} = \frac{S_{eq}}{\hbar} - \sigma_{eq} \frac{\pi}{2}, \quad \sigma_{eq} = \sigma_0 \mp \frac{1}{2}. \quad (76)$$

In all equations above, the upper and lower signs correspond to $\Delta S > 0$ (prolate case) and $\Delta S < 0$ (oblate case), respectively.

In Fig. 4 we show the oscillating part $\delta g(k)$ of the level density for a very small quadrupole deformation of $\epsilon = 0.01$, Gaussian-averaged over k with a range $\gamma = 0.6 R^{-1}$ and plotted versus the wave number $k = \sqrt{2mE}/\hbar$. Note the pronounced “supershell” oscillations that are mainly a result of the interfering triangle and square orbits [2]. In the semiclassical result (dashed line), periodic orbits with up to $N = 6$ reflections were included in the uniform approximation given by Eqs. (64,73); identical results are obtained at this deformation in the perturbative approach. Both reproduce very well the quantum-mechanical result (solid line). For details concerning the calculation of the Gutzwiller amplitudes for the equatorial and planar orbits in non-integrable axially deformed cavities, we refer to a forthcoming publication [25].

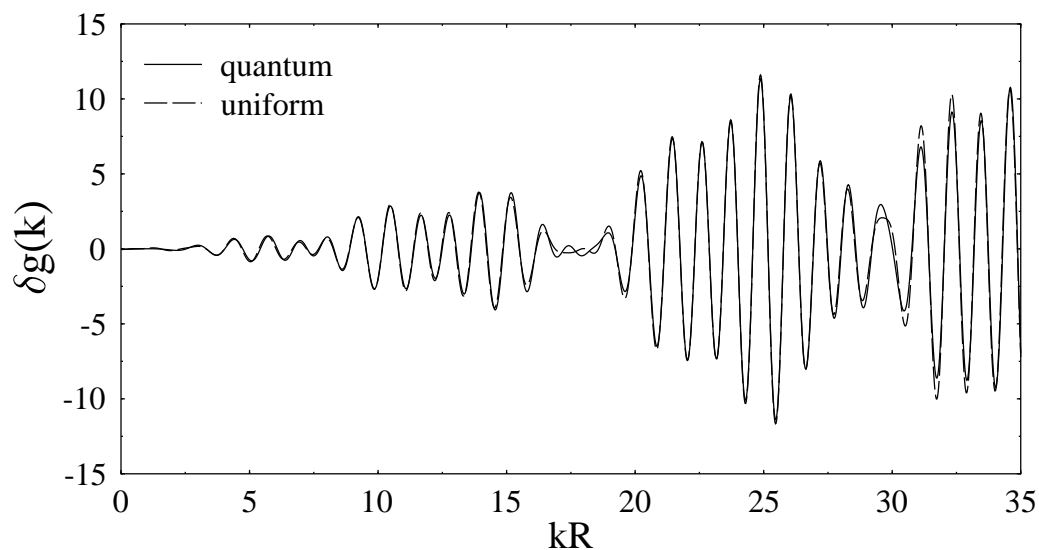


Figure 4: Oscillating part of level density in an axially-symmetric quadrupole-deformed cavity with deformation $\epsilon = 0.01$, Gaussian averaged over k with a range $\gamma = 0.6$, versus wave length k (units: R^{-1}). Solid line: quantum-mechanical result; dashed line: semiclassical result in the present uniform approximation using equatorial and planar orbits with up to $N = 6$ reflections.

In Fig. 5, we show the corresponding results at a quadrupole deformation of $\epsilon = 0.1$ at which the supershell beating is already reduced [15].

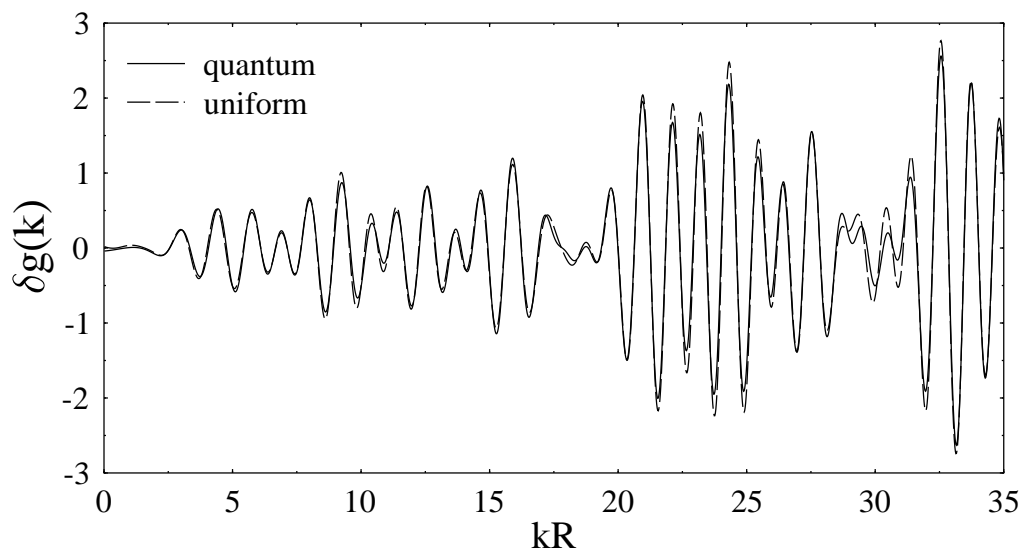


Figure 5: Same as Fig. 4, but for the deformation $\epsilon = 0.1$.

The relative importance of the different orbits at these deformations can most easily be analyzed in the Fourier spectra of the oscillating level density $\delta g(k)$. Since billiard systems exhibit scaling (i.e., the properties of the periodic orbits do not depend on energy), the Fourier

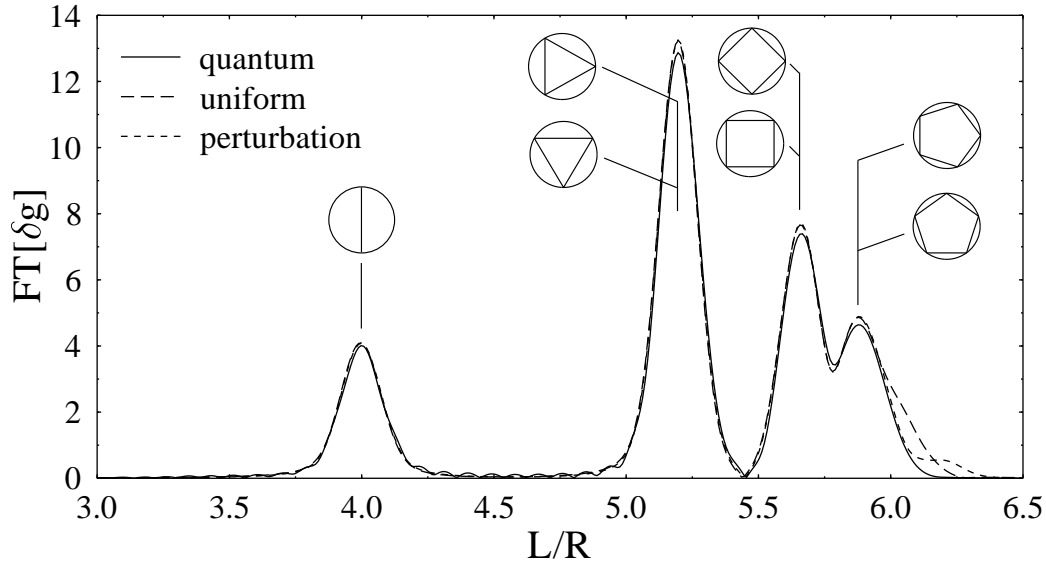


Figure 6: Fourier transform of the level densities shown in Fig. 4. The symbols indicate the periodic orbits corresponding to the Fourier peaks. The deformation ($\epsilon = 0.01$) is so small here that equatorial and planar orbits are not separated yet. The perturbation approach (short-dashed line) gives practically identical results as the uniform approximation (long-dashed line) and the quantum mechanics (solid line).

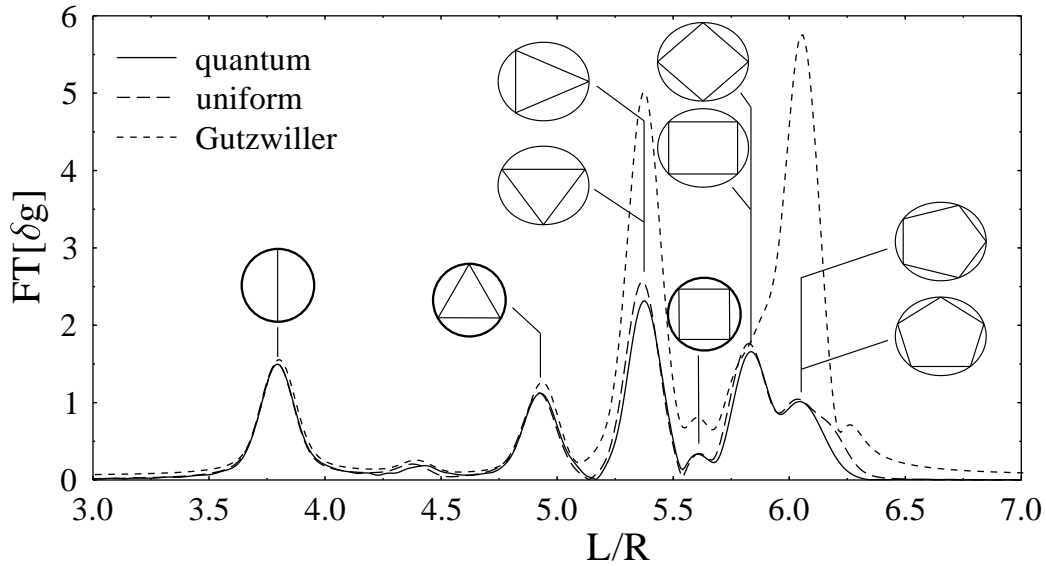


Figure 7: Fourier transform of the level densities shown in Fig. 5. At this deformation ($\epsilon = 0.1$), the equatorial orbits (symbols in heavy circles) are well separated from the planar orbits (symbols in thin ovals). However, the pairs of isolated stable and unstable planar orbits are not separated yet, as seen from the large peaks obtained with the Gutzwiller trace formula (thin-dashed line). The tiny bump at $L \simeq 4.4 R$ corresponds to the unstable isolated diameter orbit along the symmetry axis, whose Gutzwiller amplitude is smaller than all the others by a factor $\sqrt{\hbar/kR}$.

transform with respect to k gives directly power spectra in which the peaks occur at the lengths of the contributing periodic orbits. Figures 6 and 7 present the absolute values of

the Fourier transforms of the level densities shown in the above two figures. In Fig. 6, the peaks corresponding to equatorial and planar orbits cannot be separated, since at the small deformation $\epsilon = 0.01$ the spherical tori are hardly broken. Indeed, the perturbative result (short-dashed line) gives here practically identical results as the uniform approximation (long-dashed line); both agree very well with the quantum result. At the deformation $\epsilon = 0.1$, the equatorial and planar orbits are already well separated, as can be seen from Fig. 7, so that the full uniform approximation (64) for the orbits with $N \geq 3$ can here be replaced by the TGU approximation given in Eq. (68). However, the separation of the stable and unstable planar orbits is still very small. Therefore, the Gutzwiller trace formula dramatically overestimates their combined amplitudes, as seen from the short-dashed line.

5 Summary

We have derived uniform approximations for the semiclassical description of systems with perturbed $SU(2)$ and $SO(3)$ symmetry. Different from the case of bifurcations, where uniform approximations are most effectively derived from the expansion of the classical action in phase-space into normal forms [8], we use the group integral representation of the unperturbed trace formula [6] and the classical perturbation theory [14] as starting points for our development.

In terms of analytical trace formulae we can interpolate smoothly from the integrable limits to the limits where their symmetries are broken and the asymptotic Gutzwiller trace formulae for the leading periodic orbits are reached. In the two-dimensional Hénon-Heiles type potentials with broken $SU(2)$ symmetry, these orbits are isolated, whereas in the axially-symmetric quadrupole-deformed cavities with broken $SO(3)$ symmetry, they retain a one-dimensional degeneracy corresponding to the rotation about the symmetry axis. In all cases, the few shortest periodic orbits that were considered could account quantitatively for the gross-shell effects found in the coarse-grained quantum-mechanical level densities.

Unlike for the breaking of an orbit family with $U(1)$ symmetry into pairs of stable and unstable isolated orbits, for which case Tomsovic *et al.* [19] have found the universal uniform approximation given in Eq. (11), our present results for $SU(2)$ and $SO(3)$ breaking are not universal. This is due to more complicated scenarios for the breaking of rational tori that arise when more degrees of freedom, or higher-dimensional degeneracies of the orbit families, are involved. The two examples of the quartic and cubic Hénon-Heiles potentials show how the symmetry breaking can happen at different orders in the perturbation theory and lead to quite different modulation factors; see Eqs. (19) and (45) which were the starting point of our development. However, due to the feasibility of the perturbation theory and the generality of the scheme for the uniform approximation used in this study, our method can easily be applied also to other potentials and different symmetries of the unperturbed system.

We acknowledge a critical reading of the manuscript by Martin Sieber, and further helpful discussions with Ch. Amann, J. Blaschke, S. Creagh, S. Fedotkin, J. Law, and S. Tomsovic. This work has been partially supported by Deutsche Forschungsgemeinschaft (grant No. Br 733/9-1) and by Deutscher Akademischer Austauschdienst (DAAD).

A Analytical results for linear periodic orbits

For the test of numerical routines that solve the equations of motion and determine the actions of periodic orbits, it might be helpful to compare with analytical results where available. The straight-line librating periodic orbits in the Hénon-Heiles potentials allow for an analytic calculation of their actions or periods. We give here the results and a brief sketch of their derivations.

A.1 The A_1 and A_2 orbits in the quartic Hénon-Heiles potential

The potential

$$V(r, \theta) = \frac{1}{2} \omega^2 r^2 - \frac{\alpha}{4} r^4 \cos(4\theta), \quad (77)$$

has two pairs of linear librating orbits: the A_1 orbits oscillating along the x and y axes ($\theta = 0$ and $\pi/2$), and the orbits A_2 oscillating along the diagonals ($\theta = \pi/4$ and $3\pi/4$). We scale the potential with the factor $1/E^* = 4\alpha/\omega^4$, so that the equations for their classical turning points are

$$e = 2x^2 \mp x^4 \quad (78)$$

in terms of the scaled energy e (17) and the scaled radial coordinate $x = r\sqrt{\alpha}/\omega$. The upper and lower sign in (78) holds for the orbits A_1 and A_2 , respectively. The four solutions of Eq. (78) with the “−” sign are given by $\pm x_1$ and $\pm x_2$, where

$$x_1 = \sqrt{1 - \sqrt{1 - e}}, \quad x_2 = \sqrt{1 + \sqrt{1 - e}}, \quad (79)$$

and $\pm x_1$ are the classical turning points of the A_1 orbits. Their action is then

$$S_{A_1} = 8\sqrt{2} \frac{E^*}{\omega} \int_0^{x_1} \sqrt{(e - 2x^2 + x^4)} dx = 8\sqrt{2} \frac{E^*}{\omega} \int_0^{x_1} \sqrt{(x_1^2 - x^2)(x_2^2 - x^2)} dx \quad (80)$$

which can be expressed in term of the complete elliptic integrals $\mathbf{K}(t) = F(\pi/2, t)$ and $\mathbf{E}(t) = E(\pi/2, t)$ in terms of the quantity

$$t = \left(\frac{x_1}{x_2} \right)^2 = \frac{1 - \sqrt{1 - e}}{1 + \sqrt{1 - e}}. \quad (81)$$

The result is

$$S_{A_1}(e) = \frac{16\sqrt{2}}{3} \frac{E^*}{\omega} \sqrt{1 + \sqrt{1 - e}} \left[\mathbf{E}(t) - \sqrt{1 - e} \mathbf{K}(t) \right]. \quad (e < 1) \quad (82)$$

At $e = 1$ we get simply $S_{A_1}(1) = 16\sqrt{2} E^*/(3\omega)$.

For the A_2 orbits, the solutions of Eq. (78) with the “+” sign are given by $\pm x_1$ and $\pm i x_2$, where now,

$$x_1 = \sqrt{\sqrt{1 + e} - 1}, \quad x_2 = \sqrt{\sqrt{1 + e} + 1}, \quad (83)$$

and $\pm x_1$ are again the classical turning points. The action of the A_2 orbits is then

$$S_{A_2} = 8\sqrt{2} \frac{E^*}{\omega} \int_0^{x_1} \sqrt{(x_2^2 + x^2)(x_1^2 - x^2)} dx \quad (84)$$

which becomes

$$S_{A_2}(e) = \frac{16}{3} \frac{E^*}{\omega} (1+e)^{1/4} \left[(1 + \sqrt{1+e}) \mathbf{K}(\kappa) - 2 \mathbf{E}(\kappa) \right], \quad (85)$$

in terms of the quantity

$$\kappa = \frac{x_1^2}{(x_1^2 + x_2^2)} = \frac{\sqrt{1+e} - 1}{2\sqrt{1+e}}. \quad (86)$$

Taylor expansion of Eqs. (82,85) in powers of e leads to the result given in Eq. (25).

A.2 The A orbit in the standard Hénon-Heiles potential

The potential

$$V(r, \theta) = \frac{1}{2} \omega^2 r^2 - \frac{\alpha}{3} r^3 \cos(3\theta) \quad (87)$$

has linear librating orbits A oscillating along the symmetry axes ($\theta = 0, 2\pi/3$ and $4\pi/3$). We scale the potential with the factor $1/E^* = 6\alpha^2/\omega^6$, so that the equation for the classical turning points is

$$e = 3x^2 - 2x^3 \quad (88)$$

in terms of the scaled energy $e = E/E^*$ and the scaled radial coordinate $x = r\alpha/\omega^2$. The real solutions for this cubic equation for $e \leq 1$ are, with $x_1 \leq x_2 \leq x_3$,

$$x_1 = \frac{1}{2} - \cos(\pi/3 - \phi/3), \quad x_2 = \frac{1}{2} - \cos(\pi/3 + \phi/3), \quad x_3 = \frac{1}{2} + \cos(\phi/3), \quad (89)$$

where

$$\cos \phi = 1 - 2e. \quad (90)$$

The action of the A orbit is then

$$S_A = 4\sqrt{3} \frac{E^*}{\omega} \int_{x_1}^{x_2} \sqrt{e - 3x^2 + 2x^3} dx = 4\sqrt{6} \frac{E^*}{\omega} \int_{x_1}^{x_2} \sqrt{(x - x_1)(x_2 - x)(x_3 - x)} dx, \quad (91)$$

but we could not find an analytical expression for this integral. Instead, we calculate the period $T_A = dS_A/dE$

$$T_A = \frac{\sqrt{6}}{\omega} \int_{x_1}^{x_2} \frac{1}{\sqrt{(x - x_1)(x_2 - x)(x_3 - x)}} dx \quad (92)$$

which again can be expressed in terms of a complete elliptic integral by

$$T_A(e) = \frac{\sqrt{6}}{\omega} \frac{2}{\sqrt{x_3 - x_1}} \mathbf{K}(q), \quad (e < 1) \quad (93)$$

where

$$q = \left(\frac{x_2 - x_1}{x_3 - x_1} \right). \quad (94)$$

(Note that T_A diverges at $e = 1$.) Expansion of (93) in powers of e and integrating over the energy E leads to the result given in Eq. (47).

References

- [1] M. C. Gutzwiller, J. Math. Phys. **12**, 343 (1971); *Chaos in Classical and Quantum Mechanics* (Springer Verlag, New York, 1990).
- [2] R. Balian, and C. Bloch, Ann. Phys. (N. Y.) **69**, 76 (1972).
- [3] M. V. Berry and M. Tabor, Proc. R. Soc. Lond. **A 349**, 101 (1976); *ibid.* **A 356**, 375 (1977).
- [4] M. Brack and R. K. Bhaduri: *Semiclassical Physics*, Frontiers in Physics Vol. **96** (Addison-Wesley, Reading, 1997).
- [5] V. M. Strutinsky and A. G. Magner, Sov. J. Part. Nucl. **7**, 138 (1976).
- [6] S. C. Creagh and R. G. Littlejohn, Phys. Rev. A **44**, 836 (1991); J. Phys. A **25**, 1643 (1992).
- [7] P. J. Richens, J. Phys. **A 15**, 2101 (1982).
- [8] M. Sieber, J. Phys. A **29**, 4716 (1996); M. Sieber, J. Phys. **A 30**, 4563 (1997); H. Schomerus and M. Sieber, **A 30**, 4537 (1997).
- [9] M. Sieber, J. Phys. **A 30**, 4563 (1997).
- [10] A. M. Ozorio de Almeida and J. H. Hannay, J. Phys. **A 20**, 5873 (1987); see also A. M. Ozorio de Almeida: *Hamiltonian Systems: Chaos and Quantization* (Cambridge University Press, Cambridge, 1988).
- [11] A. G. Magner, S. N. Fedotkin, F. A. Ivanyuk, P. Meier, M. Brack, S. M. Reimann, and H. Koizumi, Ann. Physik (Leipzig) **6**, 555 (1997); A. G. Magner, S. N. Fedotkin, F. A. Ivanyuk, P. Meier, and M. Brack, Czech. J. Phys. **48**, 845 (1998).
- [12] Ozorio de Almeida, in *Quantum Chaos and Statistical Nuclear Physics* (T. H. Seligmann and H. Nishioka, Eds.) Lecture Notes in Physics **263**, p. 197 (Springer Verlag, New York/Berlin, 1986).
- [13] D. Ullmo, K. Richter and R. A. Jalabert, Phys. Rev. Lett. **74**, 383 (1995); see also K. Richter, D. Ullmo and R. A. Jalabert, Phys. Rep. **276**, 1 (1996).
- [14] S. C. Creagh, Ann. Phys. (N. Y.) **248**, 60 (1996).
- [15] P. Meier, M. Brack and S. C. Creagh, Z. Phys. **D 41**, 281 (1997).
- [16] M. Brack, J. Blaschke, S. C. Creagh, A. G. Magner, P. Meier, and S. M. Reimann, Z. Phys. **D 40**, 276 (1997).
- [17] K. Tanaka, S. C. Creagh and M. Brack, Phys. Rev. B **53**, 16050 (1996).
- [18] M. Brack, S. C. Creagh, and J. Law, Phys. Rev. **A 57**, 788 (1998).
- [19] S. Tomsovic, M. Grinberg and D. Ullmo, Phys. Rev. Lett **75**, 4346 (1995); see also D. Ullmo, M. Grinberg and S. Tomsovic, Phys. Rev. **E 54**, 135 (1996).
- [20] V. M. Strutinsky, A. G. Magner, S. R. Ofengenden, and T. Døssing, Z. Phys. **A 283**, 269 (1977).
- [21] M. Brack, S. M. Reimann, and M. Sieber, Phys. Rev. Lett. **79**, 1817 (1997); see also M. Brack, P. Meier, S. M. Reimann, and M. Sieber, in: *Similarities and differences between atomic nuclei and clusters*, eds. Y. Abe *et al.* (American Institute of Physics, 1998) p. 17.
- [22] H. Nishioka, K. Hansen and B. R. Mottelson, Phys. Rev. **B 42**, 9377 (1990).

- [23] K. Tanaka, Ann. Phys. (N.Y.) **268**, 31 (1998).
- [24] S. M. Reimann, M. Persson, P. E. Lindelof, and M. Brack, Z. Phys. **B 101**, 377 (1996).
- [25] P. Meier, M. Sieber, and M. Brack, to be published.
- [26] M. Brack and S. R. Jain, Phys. Rev. **A 51**, 3462 (1995).
- [27] M. Hénon and C. Heiles, Astr. J. **69**, 73 (1964).
- [28] M. Brack, R. K. Bhaduri, J. Law, M. V. N. Murthy, and Ch. Maier, Chaos **5**, 317, 707(E) (1995).
- [29] M. Abramowitz and I. Stegun: *Handbook of mathematical functions* (Dover, N.Y., 1965).